Supplementary Information

A Luminescent Cu_4 Cluster Film Grown by Electrospray Deposition: A Nitroaromatic Vapour Sensor

Arijit Jana[a], B. K. Spoorthi,[a] Akhil S. Nair,[b] Ankit Nagar,[a] Biswarup Pathak,[b]* Tomas Base[c]* and Thalappil Pradeep[a*]

[a]Department of Chemistry, DST Unit of Nanoscience (DST UNS) and Thematic Unit of Excellence (TUE), Indian Institute of Technology Madras, Chennai 600036, India. E-mail: pradeep@iitm.ac.in

[b]Department of Chemistry, Indian Institute of Technology Indore (IIT Indore), Indore 453552, India. Email: biswarup@iiti.ac.in

[c]Institute of Inorganic Chemistry, The Czech Academy of Science 1001 Husinec – Rez, 25068, Czech Republic. E-mail: tbase@iic.acs.cz

Table of Contents:

Experimental section

a) Material and chemicals

The borosilicate glass capillary (inner diameter 0.86 mm, outer diameter 1.5 mm) was purchased from Sutter instruments, USA. Platinum electrodes (99.98 % pure) of 0.2 mm diameter was bought from Sigma Aldrich, India. The *ortho*-carborane 12-iodo 9-thiol ligand was synthesized following the earlier literature, after purchasing *ortho*-carborane from Katchem s.r.o. (Czech Republic).[1, 2] Copper iodide (CuI) and sodium borohydride ($NaBH_4$, 99%) were purchased from Sigma Aldrich chemicals. 1, 2-bis(diphenylphosphino)-ethane (DPPE) was bought from Rankem chemicals. Milli-Q water was used for the purification of the cluster and electrospray deposition process. 2-nitrotoluene, 2,4-dinitrotoluene, and picric acid were purchased from Sd Fine Chem Ltd., HiMedia Lab. Pvt. Ltd., and MOLYCHEM, respectively. HPLC-grade solvents such as dichloromethane, chloroform, acetonitrile, methanol, ethanol, cyclohexane, toluene, benzene, THF, ethylacetate, and acetone were purchase from Rankem chemicals and Finar chemicals. All the chemicals are commercially available and used without further purification.

b) Synthesis of Cu_{18} nanocluster

The $[Cu_{18}(DPPE)_6H_{16}]^{2+}$ nanocluster have been synthesized by following literature report.[3] In brief, 95 mg copper iodide was mixed with 120 mg 1, 2-bis(diphenylphosphino)-ethane (DPPE) ligand in an argon closed Schleck tube. 20 ml acetonitrile was added with it. After 20 min stirring, a white suspension formed due to formation of copper phosphine complex. 187 mg $NaBH_4$ was added to the reaction mixture directly for the reduction. After 5 h reaction as formed orange color suspension confirms the formation of Cu_{18} nanocluster (shown in Fig. S1). Centrifugation of the suspended product followed by repetitive washing using methanol and acetonitrile leads to the purified product. Purified cluster extracted in DCM was used for Cu_4@ICBT synthesis. The Cu_{18} has a broad UV-vis absorption spectrum and the characteristic mass spectrum (presented in Fig. S1c, d) confirms the cluster. The yield of the product is 70 % in terms of copper.

c) Synthesis of Cu_4@ICBT nanocluster

The Cu_4@ICBT was synthesized following a ligand exchange induced structural transformation (LEIST) reaction starting from Cu_{18}. Purified Cu_{18} cluster (50 mg) in 15 ml DCM was reacted with 40 mg of *ortho*-carborane 12-iodo 9-thiol (I_9) ligand. After 2 h of reaction Cu_4@ICBT formed as a snow-white precipitates having characteristic orange emission under UV lamp (shown in Fig. S1f, g). The precipitates are extracted through ultracentrifugation. Repetitive washing using DCM and methanol removes the excess ligands. The purified cluster was dissolved in acetone for ESD process. The yield of the product is 80 % in terms of Cu_{18}.

d) Preparation of microcrystalline sample

To prepare the uniform microcrystalline powder, we have dissolved 30 mg freshly prepared cluster in 10 ml acetone. 7 ml DCM mixed with it and put for crystallization at room temperature

(25 °C). After 24, a yellowish precipitates formed bottom of the crystallization vial. After centrifugation at 1000 rpm, we have drop casted the precipitates on a glass slide for further studies. The length of these rhombus shaped microcrystal is 20-25 µm and width 5-8 µm (shown in Fig. S11b).

Theoretical calculation

The DFT calculations are carried out using Vienna Ab-Initio Simulation Package (VASP) employing GGA-PBE method.[4] Projector augmented wave (PAW) method is used for treating ion electron interactions.[5] A convergence criteria of 10^{-4} eV for minimum energy and 0.05 eV $Å^{-1}$ for Hellmann-Feynman forces on atoms are used for the calculations. The Brillouin zone was sampled at the Gamma point (1×1×1). All calculations are performed with spin polarization. The dispersion interactions were accounted for by using the DFT-D3 method.[6] The charge density difference (Δρ) of 2-NT binding at Cu_4@ICBT, is calculated by the following equation:

$$\Delta\rho = \rho_{Cu4@ICBT+2\text{-}NT} - \rho_{Cu4@ICBT} - \rho_{2\text{-}NT}$$

Where, $\rho_{Cu4@ICBT+2\text{-}NT}$, $\rho_{Cu4@ICBT}$ and $\rho_{2\text{-}NT}$ represent the charge density of 2-NT adsorbed Cu_4@ICBT, Cu_4@ICBT and 2-NT, respectively at the DFT optimized geometry.

Instrumentation

a) Electrospray deposition

Electrospray deposition experiments were performed using a home built setup. A schematic representation of the ESD setup is presented in the Fig. 1b. Charged microdroplets of Cu_4@ICBT ions were generated from a capillary tip. These tips were made by pulling the borosilicate glass capillary using a flaming micropipette puller instrument (model P-97, Sutter instrument). The diameter of the ESD tip is 25-30 µm (shown in Fig. S2). All the ESD tips were checked using an optical microscope to generate uniform microdroplets. 4-5 mg purified sample dissolved in 1 ml acetone was used for ESD process. Cluster solution was inserted inside the capillary using a microinjector pipette. A high voltage DC potential of 2.5-3 kV was applied to the solution through a platinum wire electrode (diameter 0.2 mm). Spray emitter was placed manually above the collector with tip to collector distance of 10-15 mm. After potential applied as formed spray plume consist of charged microdroplets, were directed towards ground water bath having 5-6 ml Milli-Q water inside it. A photograph of such deposition is shown in the inset of Fig. 1b.

b) Microscopic characterization

Optical microscopic images were collected using a LEICA optical microscope equipped with LAS V4.8 software in transmission mode. Optical microscopic images in the reflected mode were collected using Keyence VHX-950F digital microscope. Scanning electron microscopic (SEM) images are recorded using Verios G4 UC, Thermo Scientific field emission scanning electron microscope (FESEM). After transferring the sample on a clean aluminum foil, gold sputtering was performed to increase the conductivity of the film. All the FE SEM images were collected in high

vacuum at an operating voltage of 10-15 kV. Transmission electron microscopy (TEM) was measured using a JEOL-3010 transmission electron microscope at operating voltage of 200 kV. A Gatan 794 multiscan CCD camera was used for image collection.

c) Spectroscopic characterization

UV-vis absorption spectra were measured using Perkin Elmer Lambda 365 UV-vis spectrometer in the wavelength region of 200 to 1100 nm. Photoluminescence spectra were measured using Jobin Yvon Nanolog fluorescence spectrometer with a bandpass of 3 nm for the measurements. A CCD detector was used to record the emission intensity in the range of 300-850 nm. Film transferred on a clean glass slide was used to record the spectrum in reflectance mode. FT-IR spectra of the samples were recorded using JASCO-4100 spectrometer in attenuated total reflection (ATR) mode. Mass spectrometric studies were performed in positive ion mode using a Waters Synapt G2Si-HDMS instrument. The instrument is equipped with an electrospray source, quadrupole ion trap, ion mobility cell and time of flight (TOF) detector. Electrosprayed film was dissolved in acetone to record the spectrum. Formic acid was added to enhance the ionization. The sample was electrosprayed at a flow rate of 10 µL/min with capillary voltage 3 kV, cone voltage 0 kV, spray current 100 nA, source temperature 80 °C, desolvation temperature 100 °C and desolvation gas flow of 300 L/h for the measurement. X-ray photoelectron (XPS) spectra were measured using ESCA probe TPD (Omicron Nanotechnology) equipped with Mg Kα X-ray source (hγ =1253.6 eV). X-ray flux was adjusted to reduce the beam induced damage. At least three spectra were collected and average was taken for selected binding energy. The spectra were calibrated using the binding energy of C 1s peak at 284.8 eV. Powder X-ray diffraction of the film was measured using a D8 Advance Bruker instrument, using Cu Kα X-ray source (hγ = 8047.8 eV).

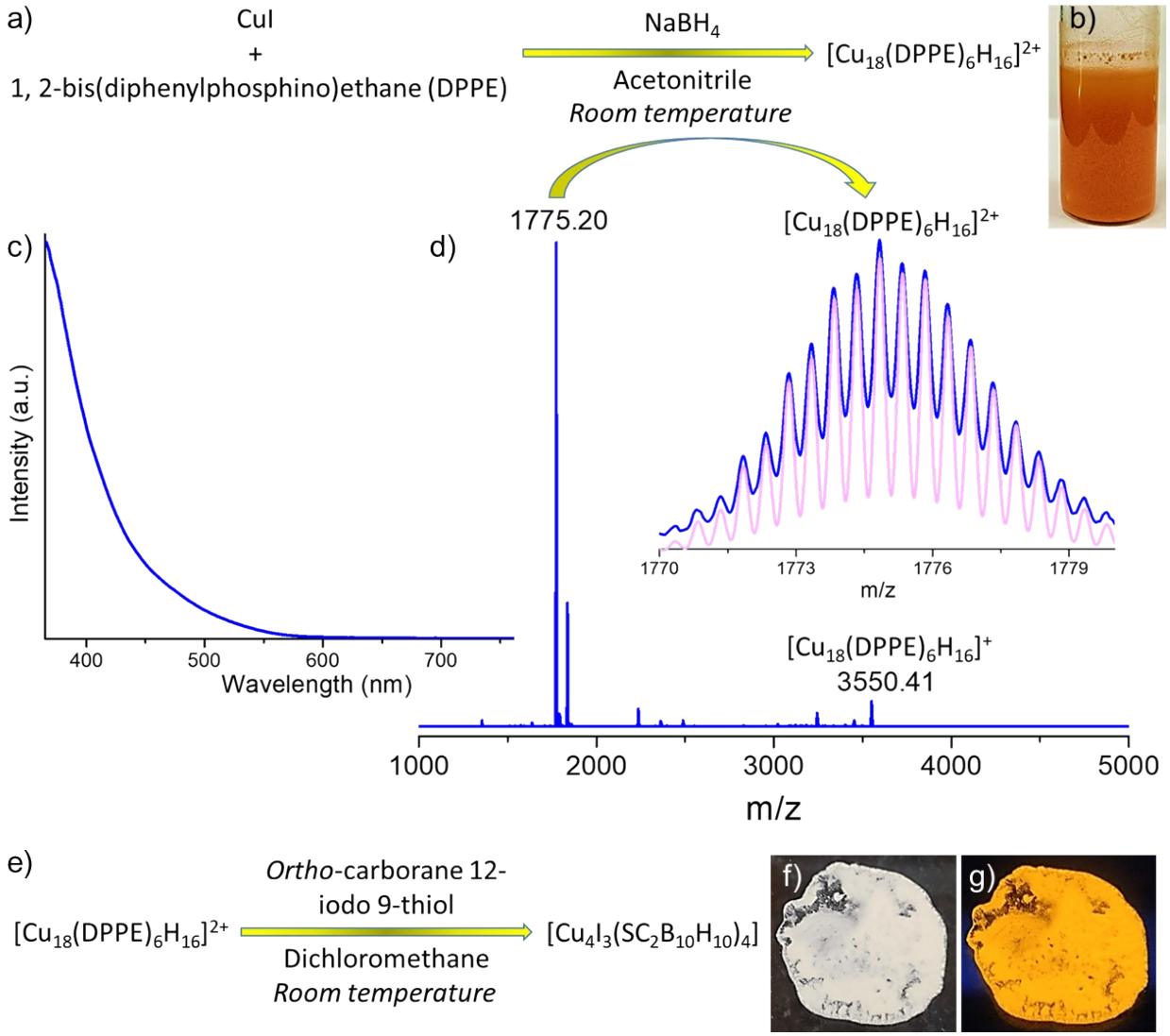

Fig. S1 a) Scheme of the synthesis of Cu_{18} through reduction reaction. b) Optical photograph of as prepared Cu_{18}. c) UV-vis absorption spectrum of the cluster. d) Mass spectrum of the cluster in positive ion mode. Both monopositive and dipositive species were observed in the spectrum. Inset shows exact matching of the isotopic distribution of the experimental (blue) with theoretical (pink) spectrum. e) Scheme of the synthesis of Cu_4@ICBT through LEIST reaction. Photographs of purified Cu_4@ICBT f) under daylight and g) under UV light. Visible orange emission was observed.

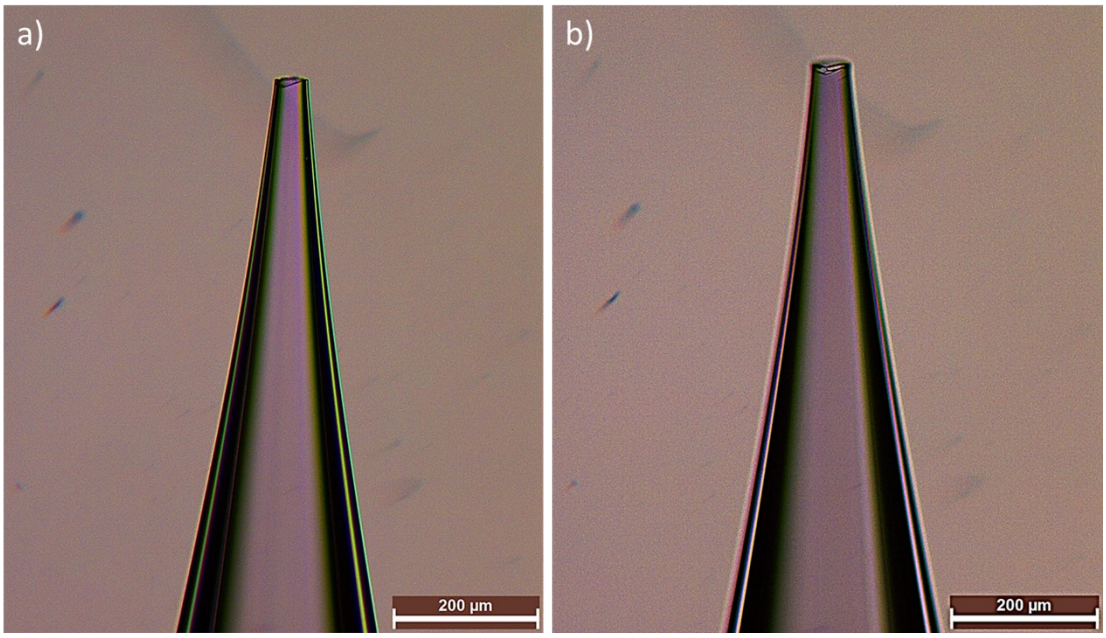

Fig. S2. a, b) Optical microscopic images of the electrospray tips, made by pulling the borosilicate glass capillary. Tip diameter is 25-30 µm.

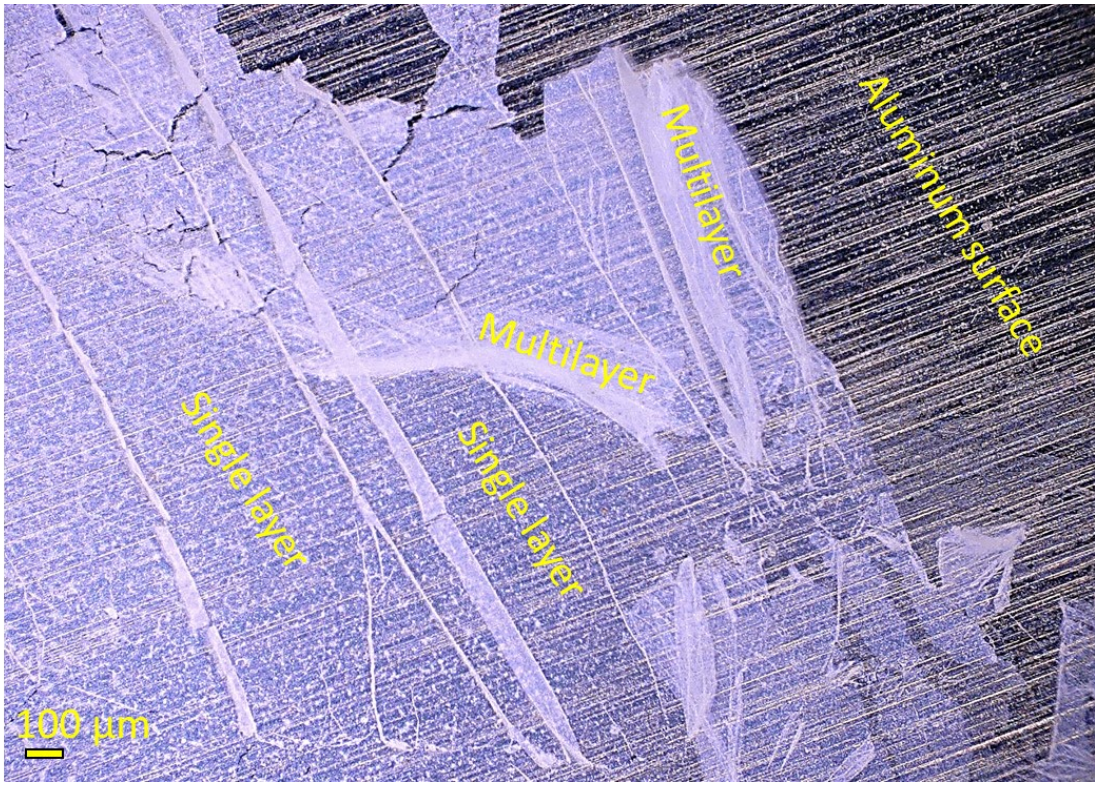

Fig. S3 Optical microscopic image of the ESD-film.

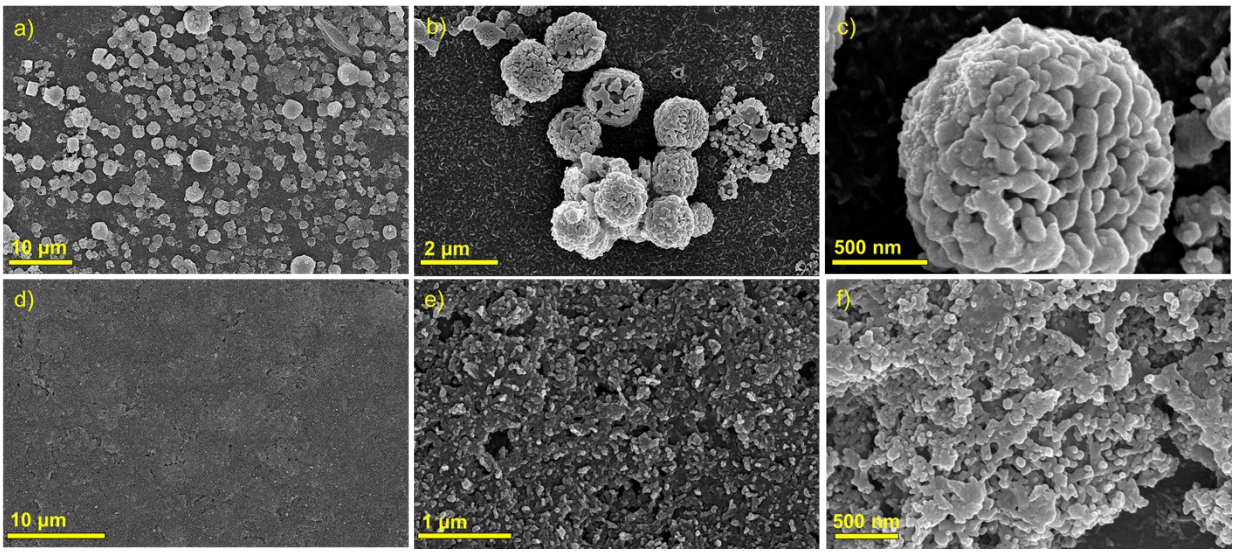

Fig. S4 FESEM micrographs showed the time dependent growth of film during ESD process, a-c) micrographs with increasing magnification after 10-15 min of ESD process, which showed the formation of spherical aggregate. d-f) micrographs of the film with increasing magnification after 30 min of ESD process.

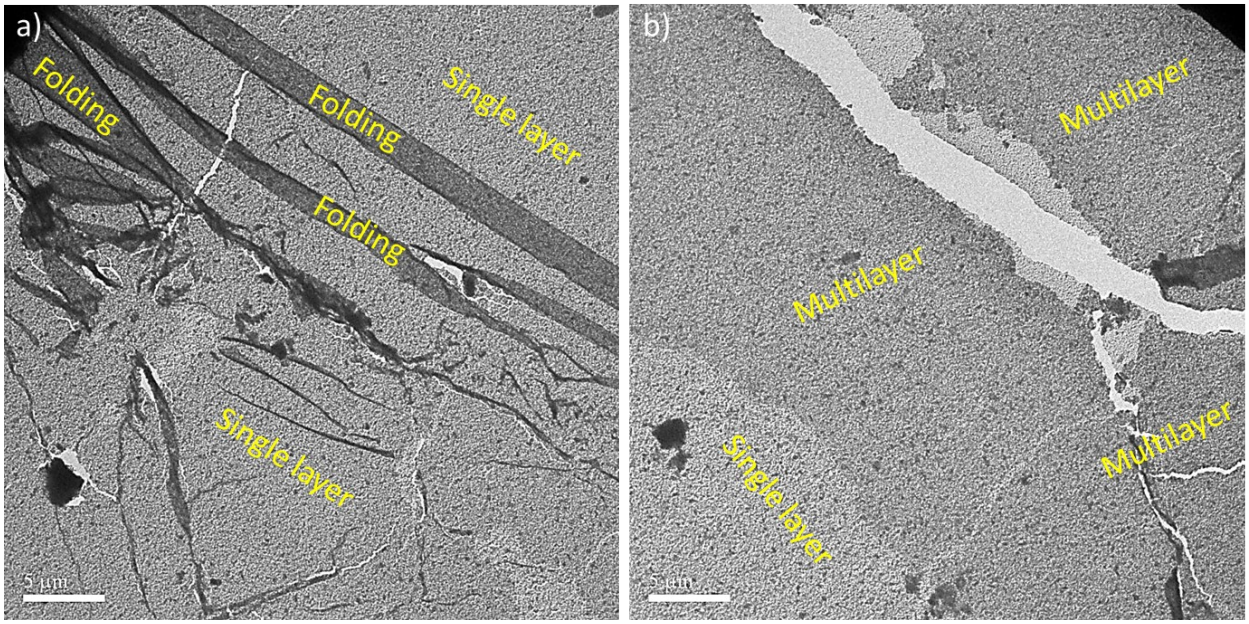

Fig. S5 a, b) TEM micrographs of different films.

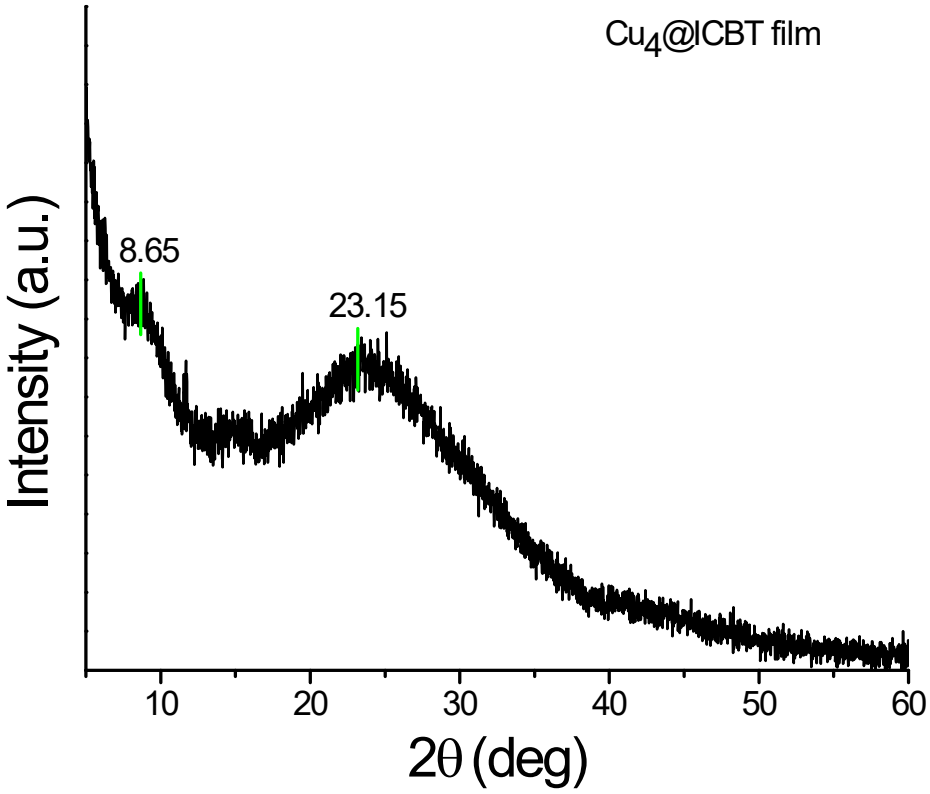

Fig. S6 Thin film XRD spectrum of the Cu_4@ICBT film having two broad diffraction features.

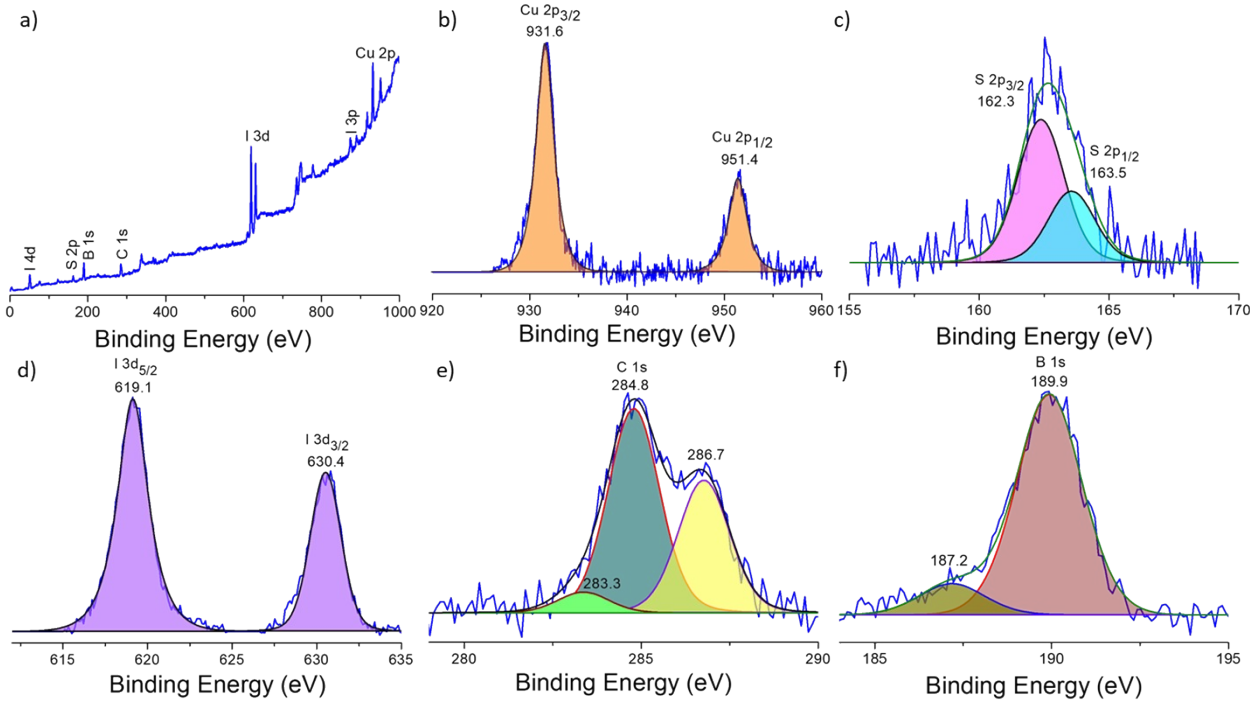

Fig. S7 a) XPS survey spectrum of Cu_4@ICBT film. Selected peak fittings of b) Cu 2p, c) S 2p, d) I 3d, e) C 1s and f) B 1s spectral regions.

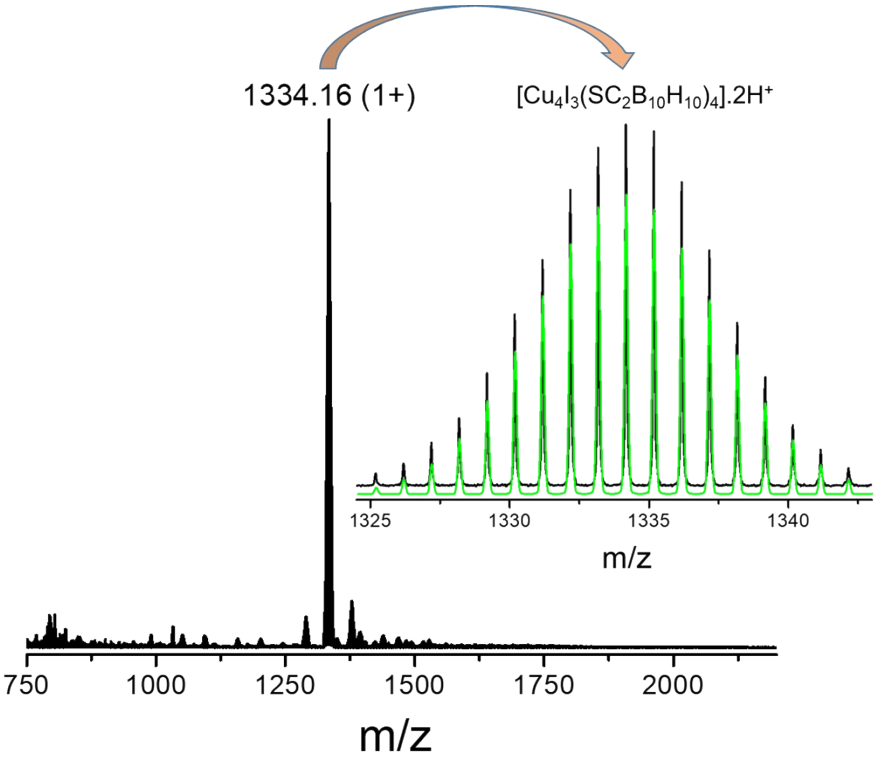

Fig. S8 High-resolution ESI-MS spectrum in positive ion mode of the ESD-film after 2-NT adsorption and desorption cycle. Isotopic distribution of the experimental spectrum (black color) at m/z 1334.16 matches well with the simulated spectrum (green color)

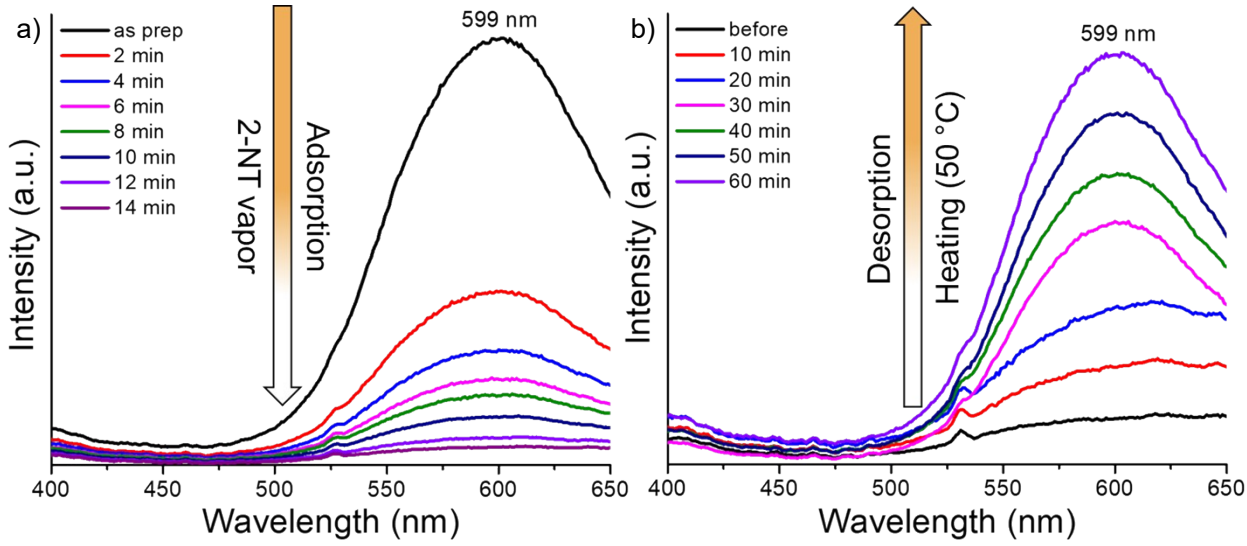

Fig. S9 Photoluminescence spectral profile of 2-NT a) adsorption and b) desorption by the Cu_4@ICBT film.

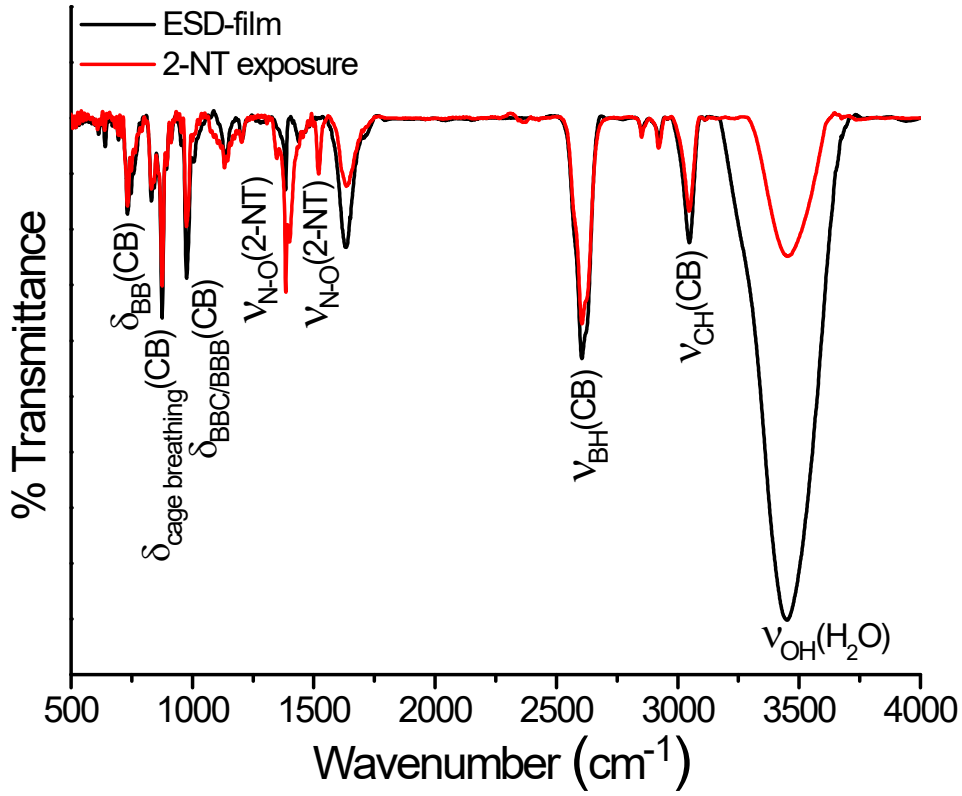

Fig. S10 Full range IR spectra of the film before and after 2-NT adsorption.

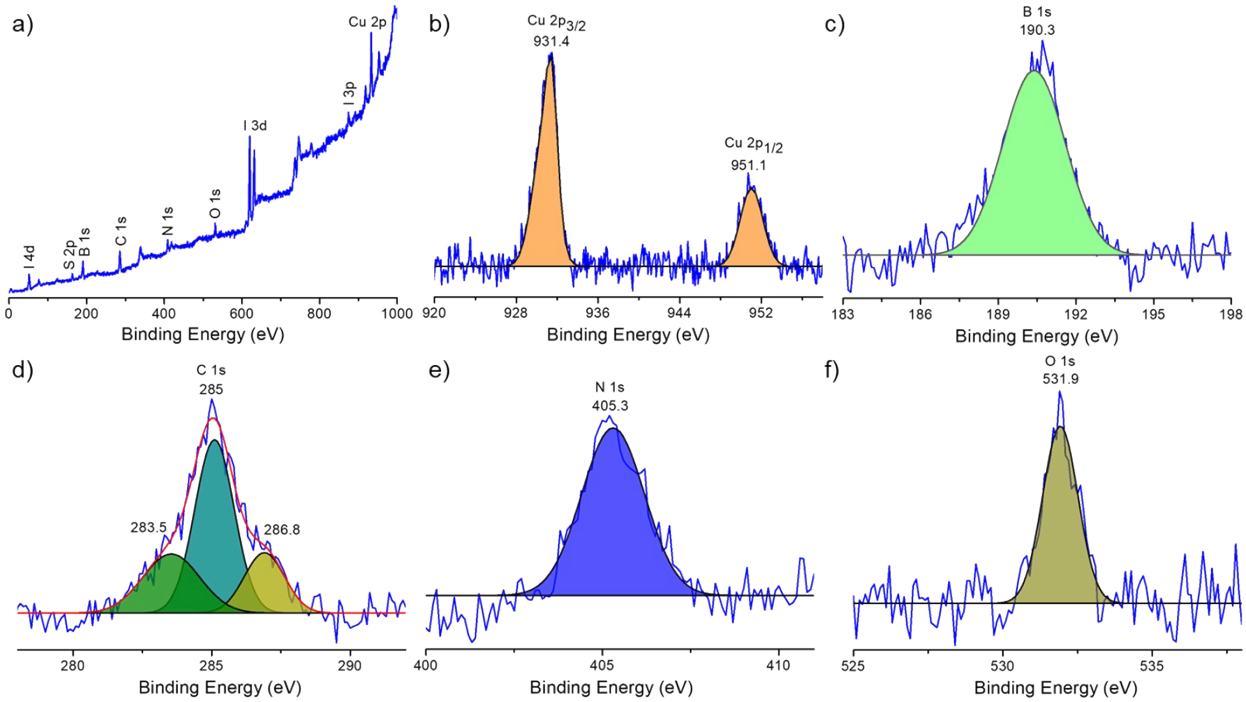

Fig. S11 XPS spectra of the Cu_4@ICBT film after 2-NT vapor exposure. a) Survey spectrum and selected peak fittings of b) Cu 2p, c) B 1s, d) C 1s, e) N 1s and f) O 1s spectral regions.

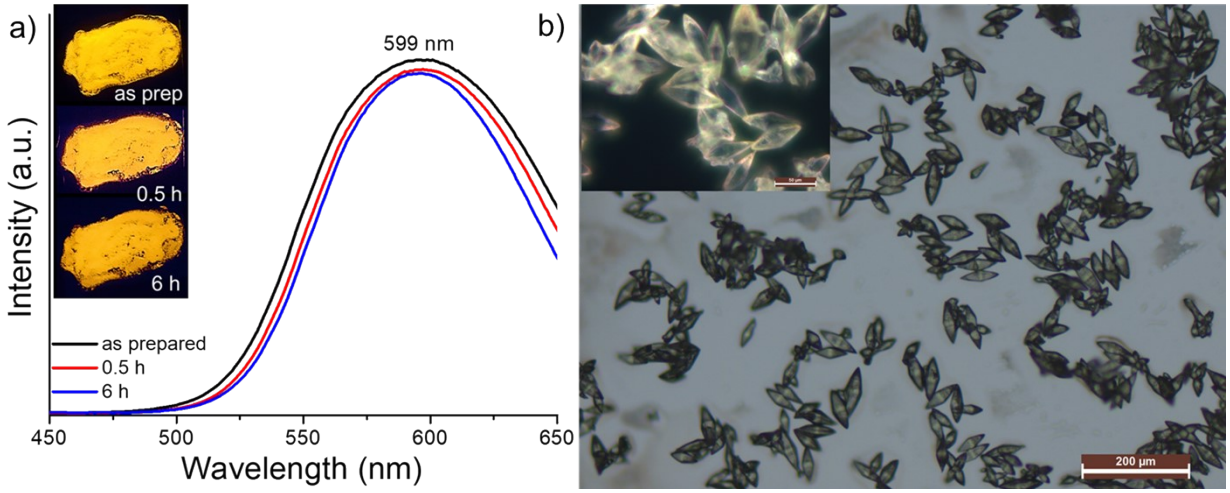

Fig. S12 a) Photoluminescence spectra shows no significant emission quenching of rhombus microcrystals upon exposure of 2-NT. Inset shows bright orange emission after 6 h 2-NT exposure. b) Optical microscopic image of the uniform rhombus microcrystals.

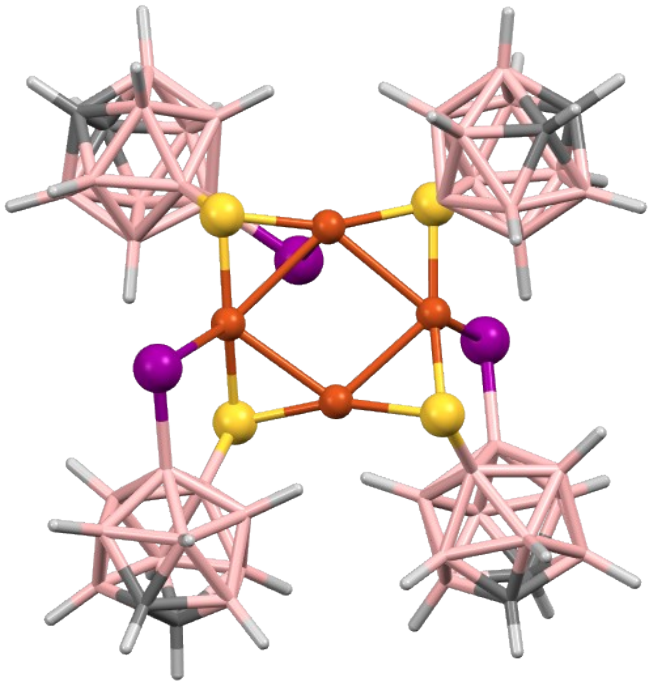

Fig. S13 DFT optimized structure of Cu_4@ICBT nanocluster having a square planer Cu_4 kernel protected by four carborane ligands. Atomic color code: orange = copper, yellow = sulphur, pink = boron, grey = carbon, violet = iodine and white = hydrogen.

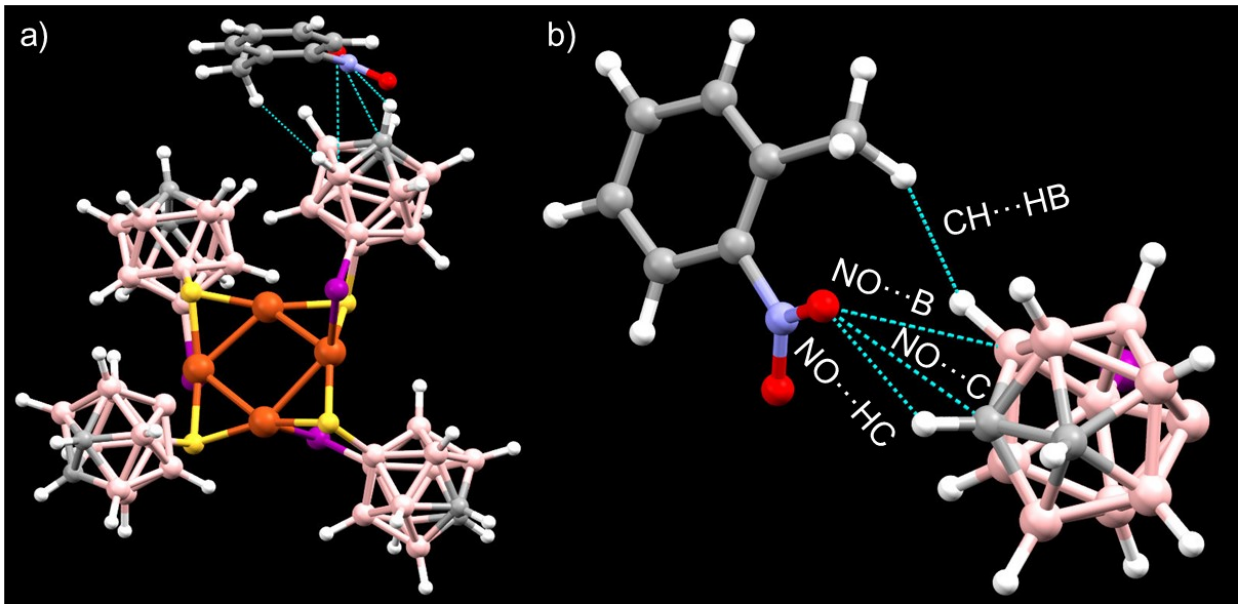

Fig. S14 a) Short contact van der Waal interactions of 2-NT with cluster in P1 configuration. b) Expanded view of these interactions.

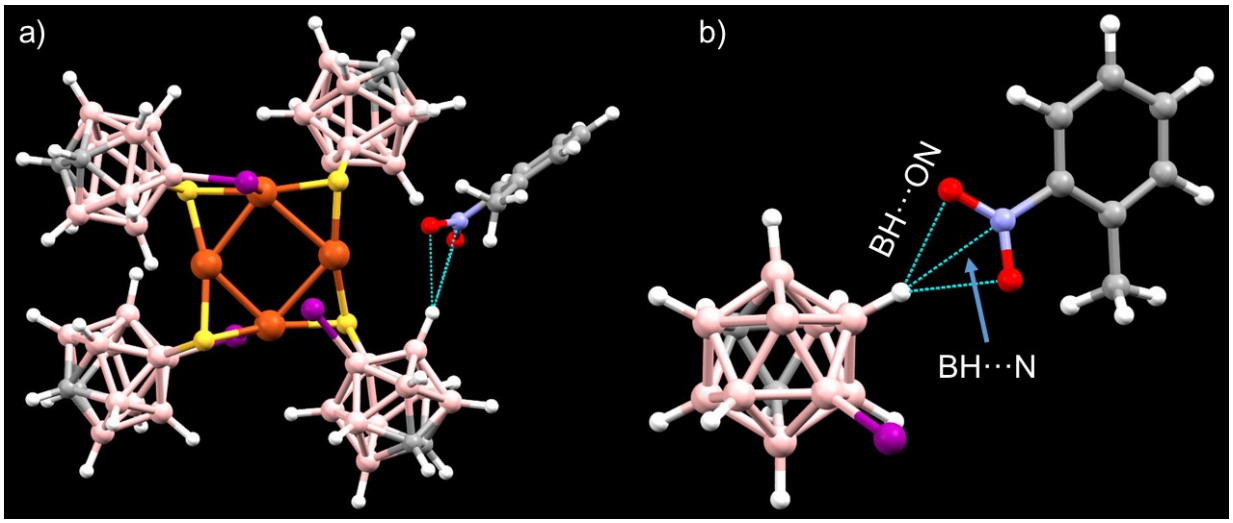

Fig. S15 a) Short contact van der Waals interactions of 2-NT with cluster in P2 configuration. b) Expanded view of these interactions.

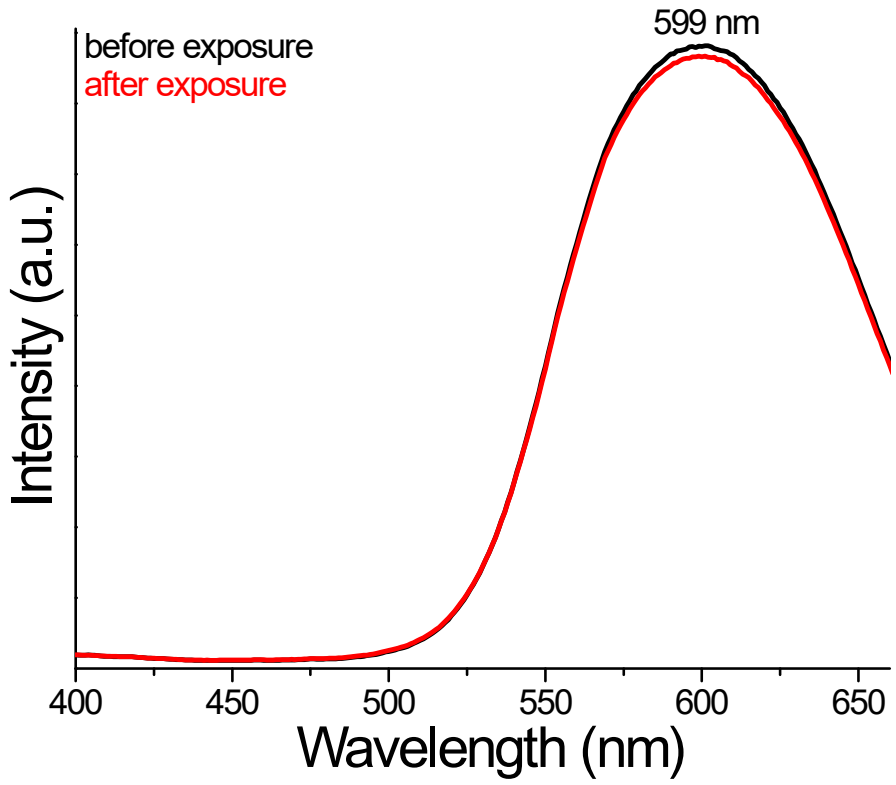

Fig. S16 PL spectra of the film before and after DCM exposure.

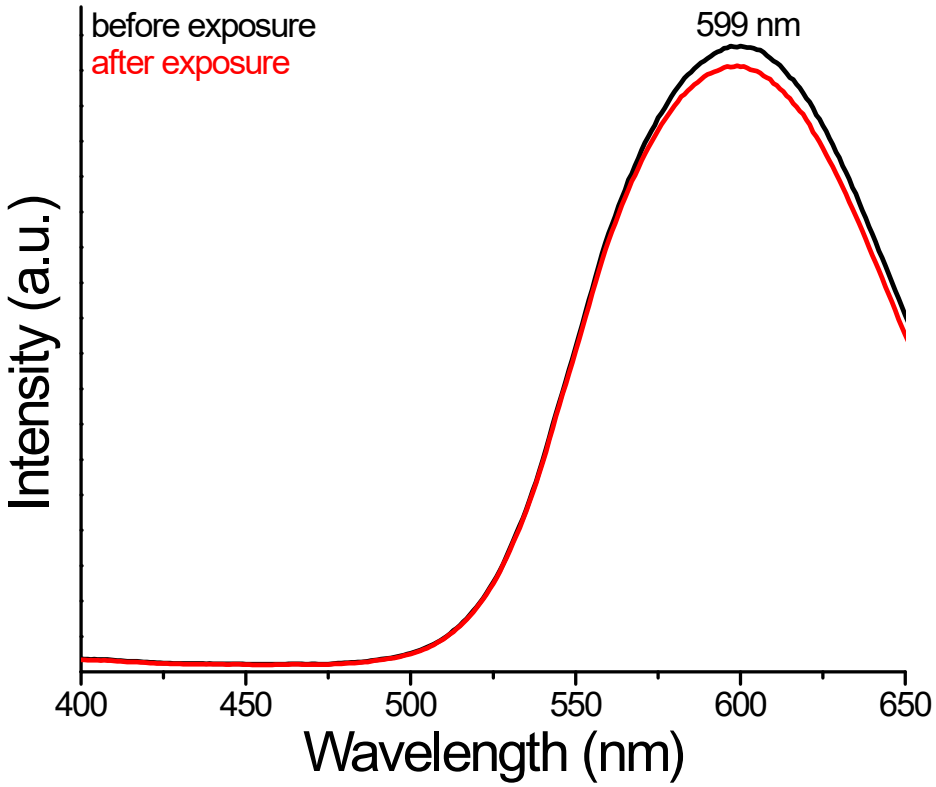

Fig. S17 PL spectra of the film before and after chloroform exposure.

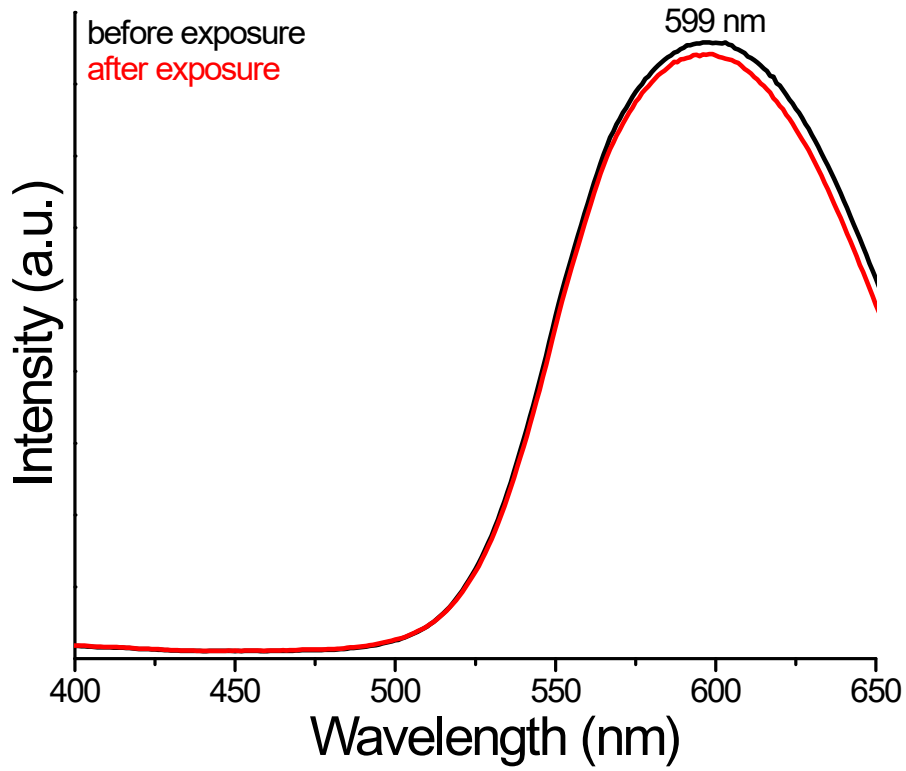

Fig. S18 PL spectra of the film before and after methanol exposure.

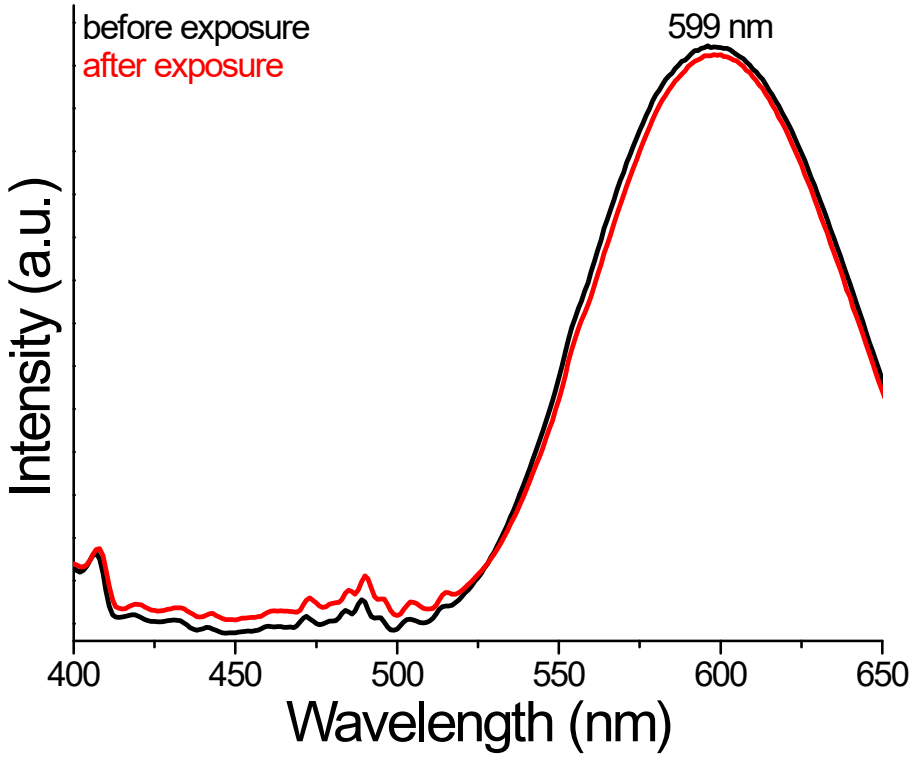

Fig. S19 PL spectra of the film before and after ethanol exposure.

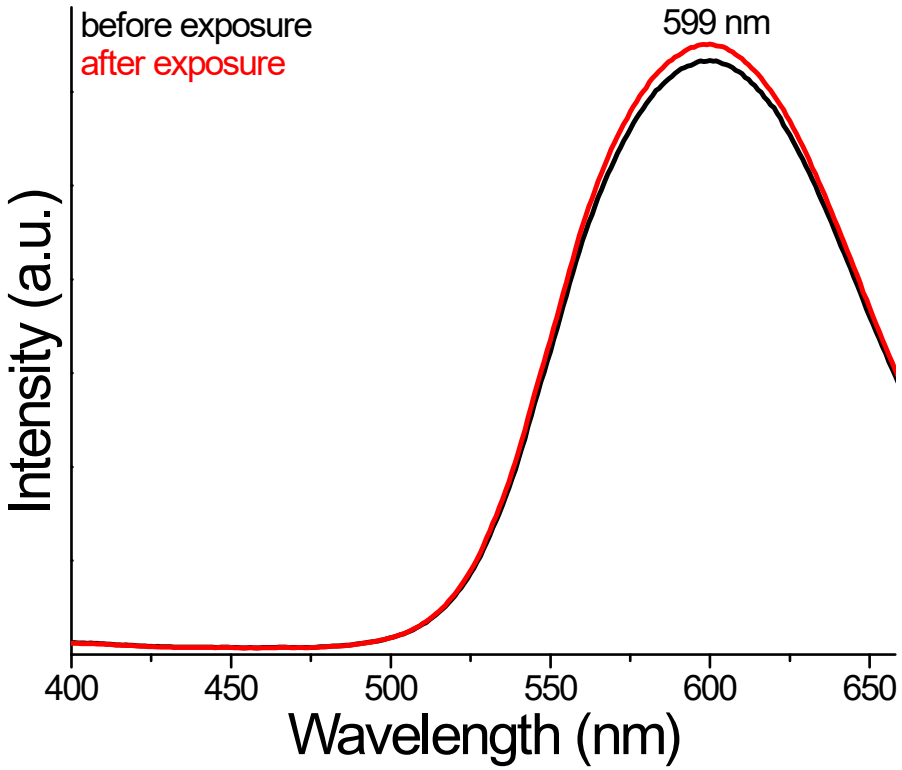

Fig. S20 PL spectra of the film before and after hexane exposure.

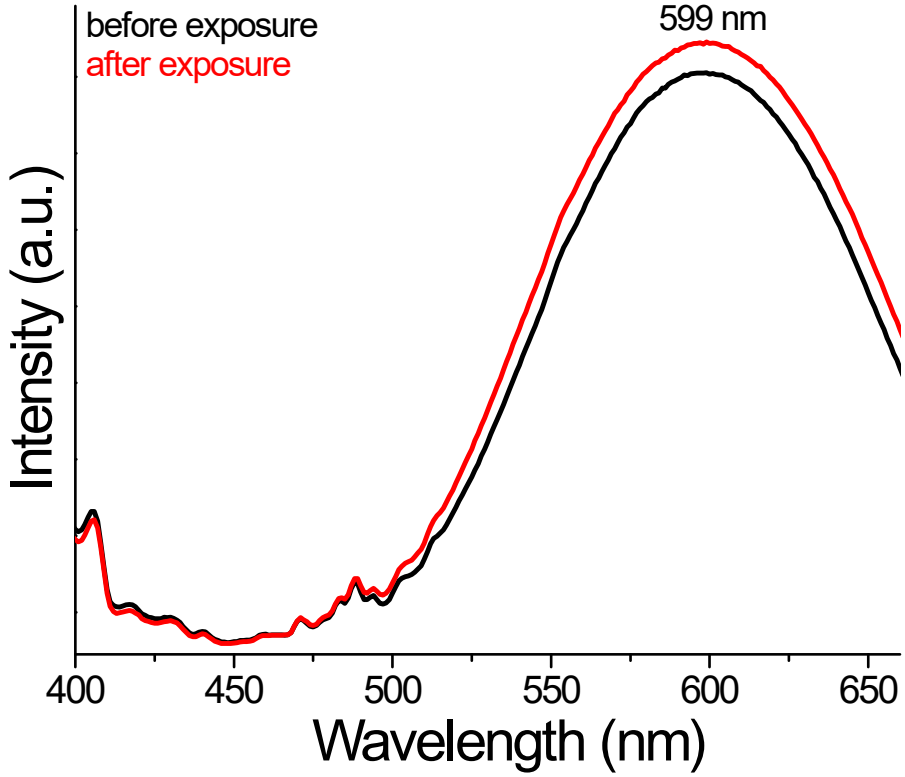

Fig. S21 PL spectra of the film before and after cyclohexane exposure.

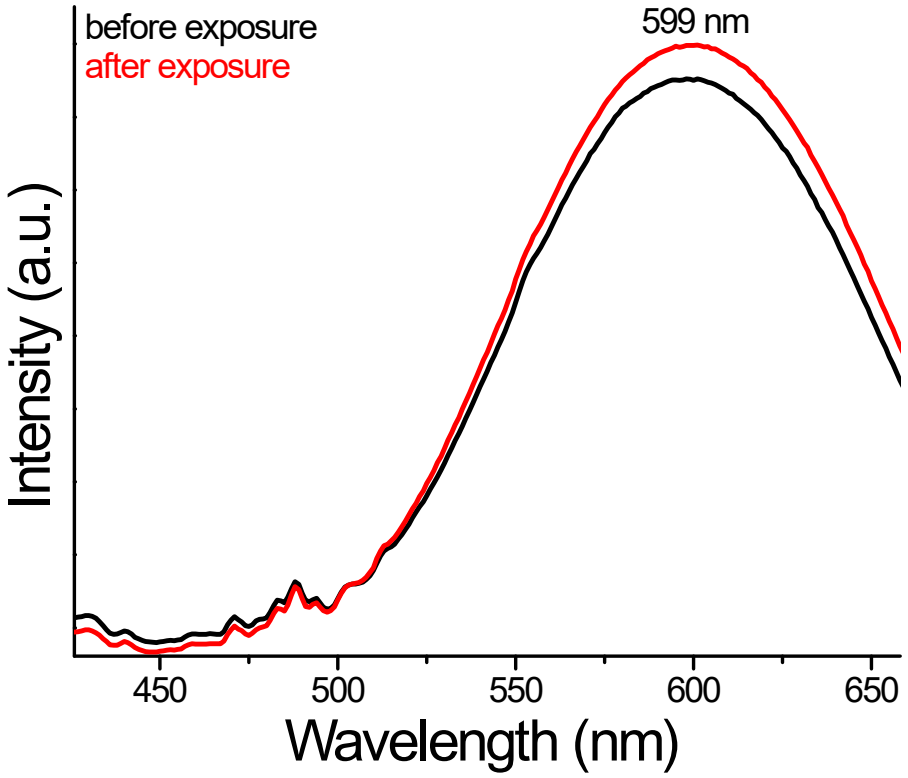

Fig. S22 PL spectra of the film before and after benzene exposure.

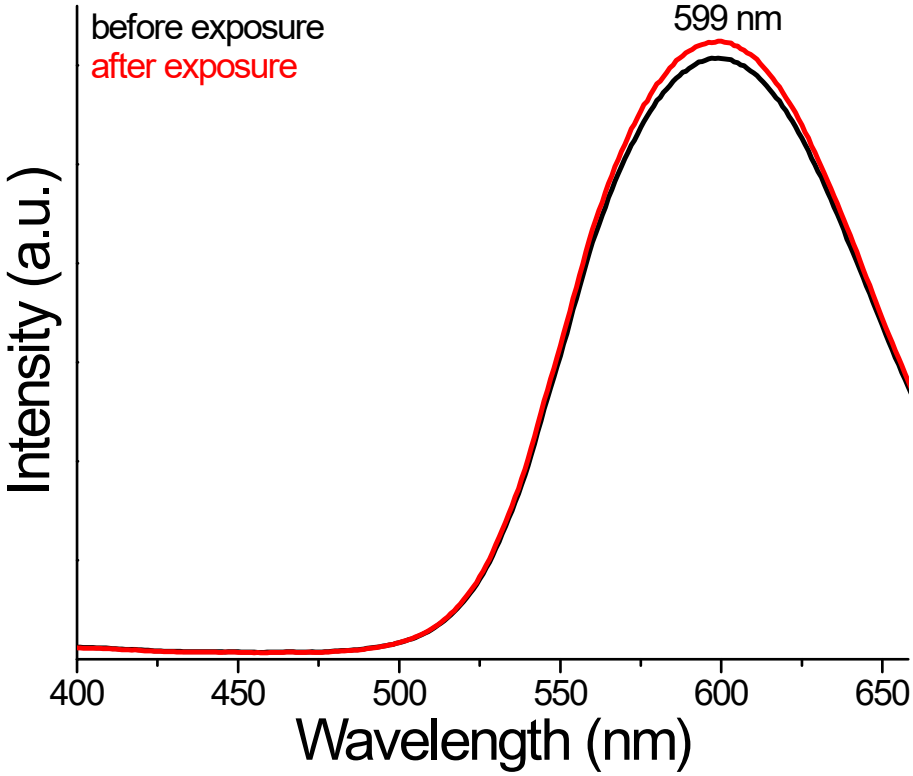

Fig. S23 PL spectra of the film before and after toluene exposure.

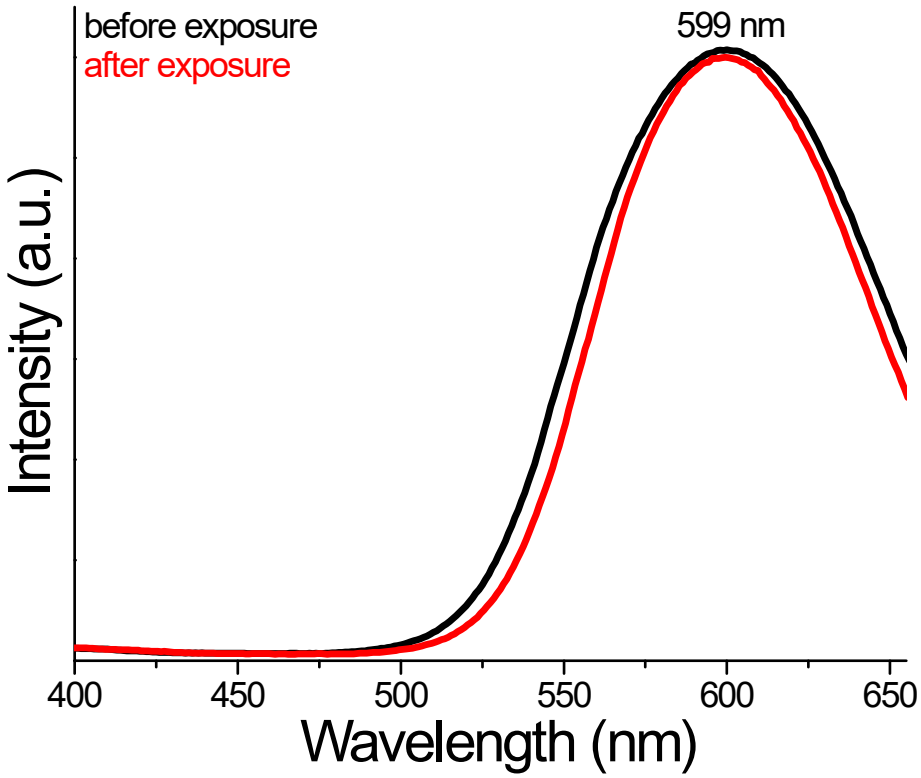

Fig. S24 PL spectra of the film before and after acetonitrile exposure.

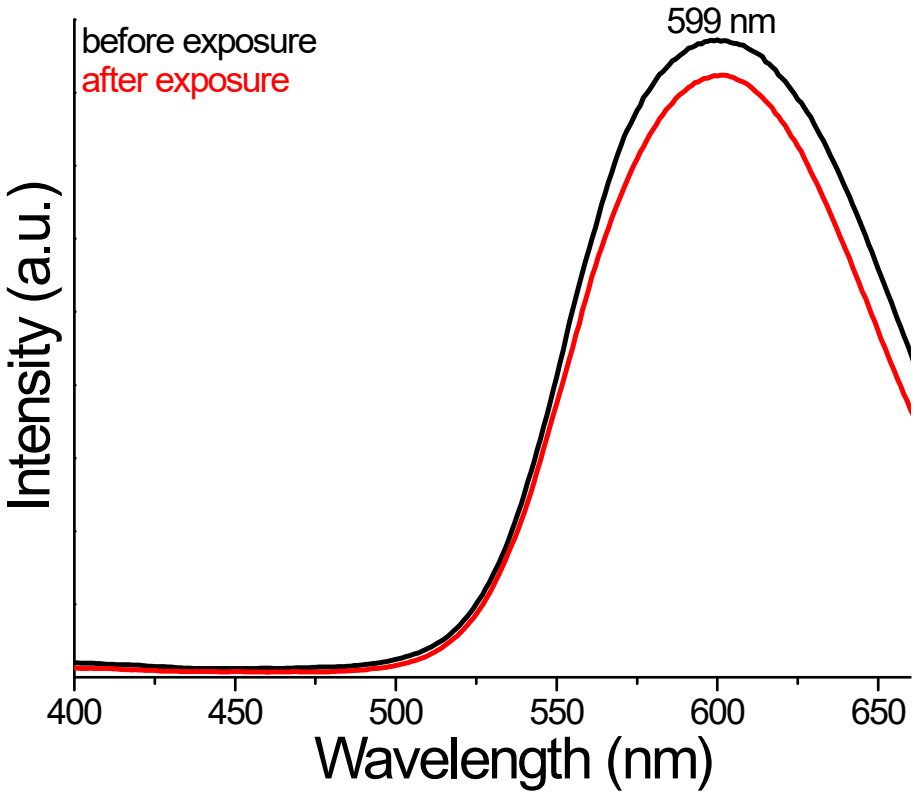

Fig. S25 PL spectra of the film before and after THF exposure.

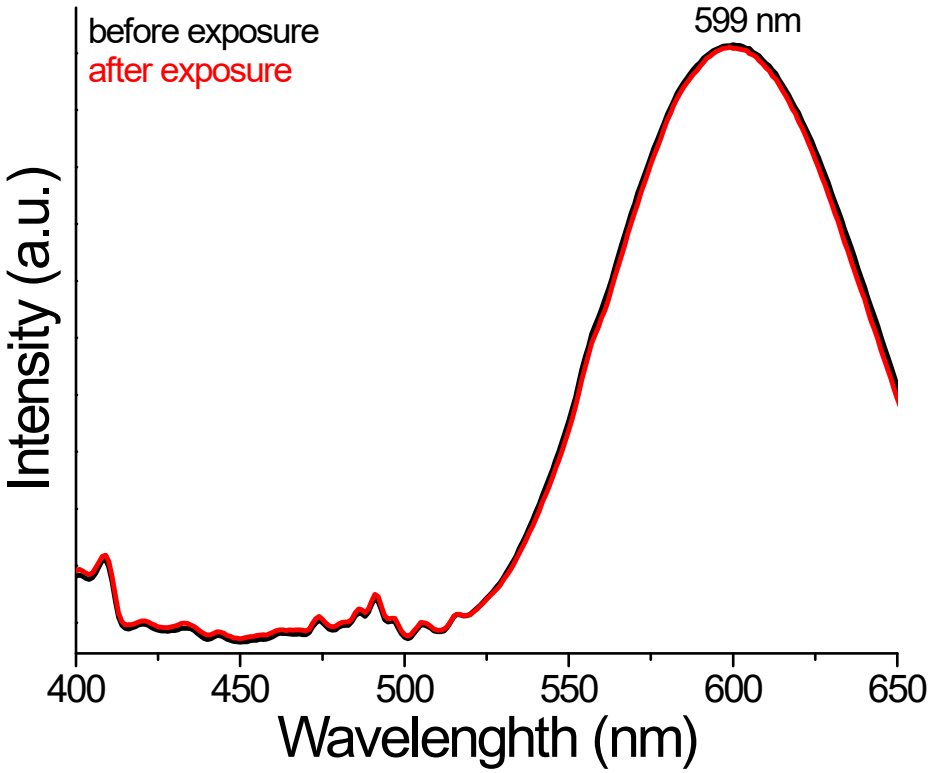

Fig. S26 PL spectra of the film before and after ethylacetate exposure.

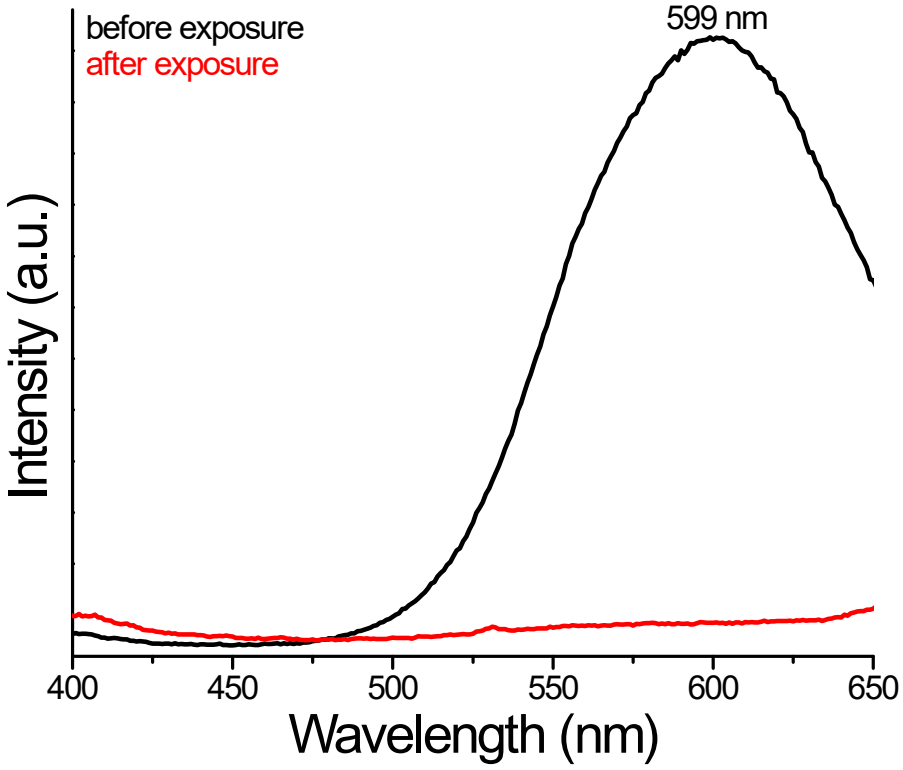

Fig. S27 PL spectra of the film before and after 2, 4-dinitrotoluene exposure.

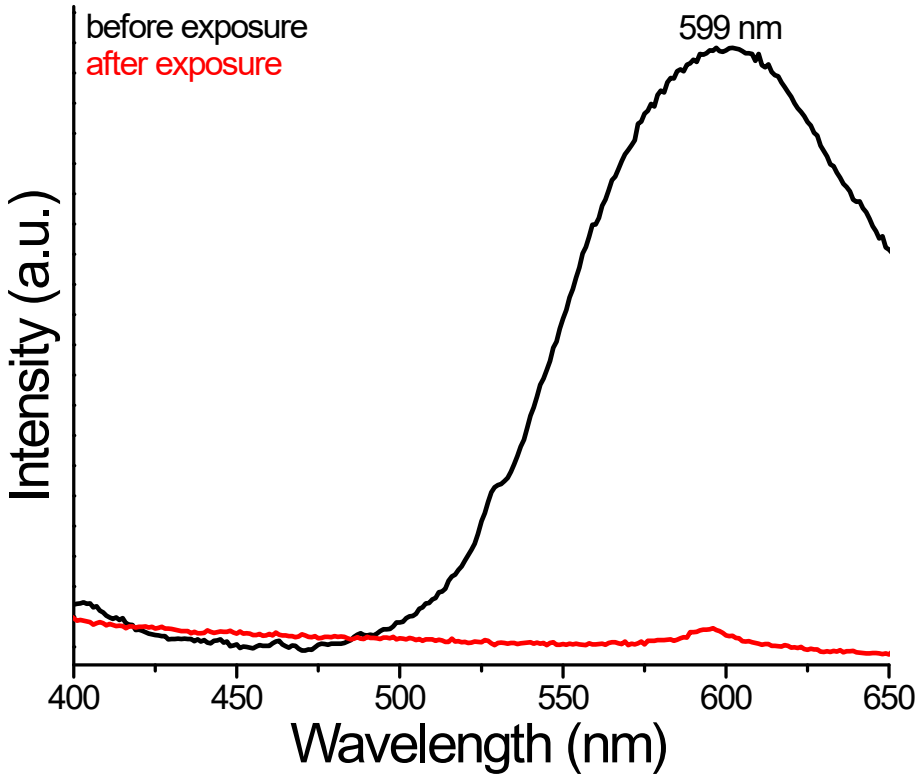

Fig. S28 PL spectra of the film before and after picric acid exposure.

References

1 J. Plešek, S. Hermanek, *Collect. Czech Chem. Commun.*, 1981, **46**, 687-692.

2 J. Plešek, Z. Janoušek, S. Hermanek, *Czech Chem. Commun.*, 1978, **43**, 1332-1338.

3 J. Li, H. Z. Ma, G. E. Reid, A. J. Edwards, Y. Hong, J. M. White, R. J. Mulder and R. A. J. O'Hair, *Chem. - A Eur. J.*, 2018, **24**, 2070–2074.

4 G. Kresse and J. Hafner, *Phys. Rev. B*, 1994, **49**, 14251–14269.

5 G. Kresse and D. Joubert, *Phys. Rev. B - Condens. Matter Mater. Phys.*, 1999, **59**, 1758–1775.

6 S. Grimme, *J. Comput. Chem.*, 2006, **27**, 1787–1799.